Heliyon 10 (2024) e29387

Contents lists available at ScienceDirect

Heliyon

journal homepage: www.cell.com/heliyon

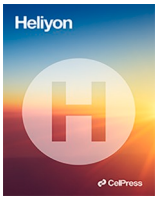

Research article

A novel model based on ubiquitination-related gene to predict prognosis and immunotherapy response in hepatocellular carcinoma

Zhiyu Chen [a,1], Jing Su [b,1], Ningning You [a], Hong Lin [a], Shanshan Lin [a], Zhenjiang Zhang [c,**], Yi Chen [a,*]

[a] Departments of Gastroenterology, Taizhou Hospital of Zhejiang Province Affiliated to Wenzhou Medical University, Taizhou, China
[b] Hematology Laboratory, Suqian First People's Hospital Affiliated to Nanjing Medical University, Suqian, China
[c] Department of Infectious Diseases, Suqian First People's Hospital Affiliated to Nanjing Medical University, Suqian, China

ARTICLE INFO

Keywords:
Hepatocellular carcinoma
Ubiquitination-related genes
Immunotherapy
Immune cells
Gene expression

ABSTRACT

Background: Hepatocellular carcinoma (HCC) is a common cancer that is increasingly becoming a global health problem and a major public health concern. In order to improve patient outcomes, additional biomarkers and targets must be explored. Ubiquitination-related genes (URGs), as tumor regulators, exhibit multiple functions in tumor development. Our objective was to examine the influence of URGs on the prognosis of patients with HCC.
Methods: By utilizing unsupervised cluster analysis, we were able to identify URGs in the database and create a risk score profile for predicting the prognosis of patients with HCC. The model's clinical application was explored using subject operating characteristic curves, survival analysis, and correlation analysis. We additionally examined the variances in clinical traits, immune infiltration, somatic genetic alterations, and responsiveness to treatment among high- and low-risk populations identified by the prognostic model. Scores for immune cell infiltration and immune-related pathway activity were determined by performing ssGSEA enrichment analysis. Additionally, to investigate potential mechanisms, we utilized GO, KEGG and GSVA analyses.
Results: We developed a risk scoring model that relies on genes associated with ubiquitination. As the risk score increased, the malignancy and prognosis of the tumor worsened. The high-risk and low-risk groups exhibited notable disparities in relation to the immune microenvironment, genes associated with immune checkpoints, sensitivity to drugs, and response to immunotherapy.
Conclusion: The utilization of a risk model that relies on genes associated with ubiquitination can serve as a biomarker to assess the prognosis of patients with HCC, and aid in the selection of suitable therapeutic agents.

1. Introduction

Hepatocellular carcinoma (HCC), as the sixth most common tumor in the world, is currently the fourth leading cause of cancer-

* Corresponding author.
** Corresponding author.
E-mail addresses: zzj77177@126.com (Z. Zhang), wzykdxchenyi@163.com (Y. Chen).
[1] Contributed equally.

https://doi.org/10.1016/j.heliyon.2024.e29387
Received 11 January 2024; Received in revised form 7 April 2024; Accepted 8 April 2024
Available online 9 April 2024

related mortality [1,2]. According to the most recent epidemiological information, HCC is closely associated with the following risk factors: infection with the hepatitis virus, exposure to Aflatoxin, non-alcoholic fatty liver disease, excessive alcohol intake, and obesity [3,4]. At present, the main treatment methods for liver cancer include surgical resection, liver spread, thermal expansion, intra-arterial, radiation and systemic therapies [5]. Although the therapeutic outcome in the majority of patients with HCC is still unsatisfactory. Hence, there is an urgent need for the identification of novel crucial genes that can serve as therapeutic targets and enhance the clinical outcomes of individuals diagnosed with HCC.

Post-translational modification (PTM) is a crucial mechanism that precisely regulates protein activity, influencing cellular metabolism and facilitating adaptation to genetic and environmental variations. Ubiquitination stands out as a pivotal PTM, essential for upholding the cellular protein homeostasis and represents a prominent focus of current research endeavors [6]. The ubiquitination pathways play a key role in regulating the anti-tumor immunity of immune cells and the immunosuppression of tumor cells in the tumor microenvironment (TME) of patients, primarily involving the DNA damage repair, p53 activation, cell cycle, and apoptosis [7,8]. In addition, targeting the ubiquitin pathway is becoming a promising cancer treatment strategy [8]. According to Zhang et al., ubiquitination related genes (URGs) serve as the standard for classifying molecular subtypes and stratifying patient risk [9]. Furthermore, several drugs depending on ubiquitin-related pathways has been approved by Food and Drug Administration (FDA) for cancer therapy [10,11].

URGs have been considered as controllers of tumors, impacting the regulation of tumor cell cycle, expression of genes, and advancement [12]. Nowadays, many scholars have applied URGs related characteristics to forecast the future course and immune reaction of various types of cancer, such as lung adenocarcinoma and endometrial cancer, the prognostic signature based on URGs performed well in predicting the infiltration of immune cells and the level of tumor mutation burden (TMB) within the TME and the effectiveness of immunotherapy for cancer treatment [13,14]. There were several studies have uncovered the relationship of URGs and the initiation and development of HCC, nevertheless, the role of URGs in HCC has not been systematically analyzed [15,16].

To investigate the correlation between URGs and the outlook of individuals with HCC, we discovered URGs in a database and created a risk score profile using unsupervised cluster analysis to forecast the prognosis of HCC patients. The model's clinical application was explored using subject operating characteristic curves, survival analysis, and correlation analysis. To offer clinical treatment guidance, we conducted a comprehensive analysis of clinical characteristics, immune infiltration, somatic mutations, and treatment sensitivity in high- and low-risk populations identified by the prognostic model. Our results indicate that URGs have served as potential prognostic biomarkers and therapeutic targets for liver cancer patients. The URGs screened and the model constructed in this study will aid in formulating liver cancer treatment strategies and provide new insights.

2. Materials and methods

2.1. Data preparation

We obtained transcriptome expression data, clinicopathologic information, somatic mutations, and copy number variation data from The Cancer Genome Atlas (TCGA) for 377 patients with hepatocellular carcinoma (https://portal.gdc.cancer.gov/). Data on 260 HCC patients from the International Cancer Genome Consortium (ICGC) were obtained as validation (https://dcc.icgc.org/). URGs were obtained from the iUUCD database (http://iuucd.biocuckoo.org/). Utilizing the TCGA dataset, we applied the "limma" R package to examine the differential expression of Upregulated Genes (URGs) (logFC >1 or logFC < -1, $P < 0.05$) between normal and tumor tissues of HCC for further exploration.

2.2. Consensus clustering analysis

Consensus clustering of HCC patients was performed using the "ConsensusClusterPlus" R package [17]. We achieved consistent results by evaluating the optimal number of clusters within the range of $k = 2$–9 over 1000 iterations. Cumulative distribution function (CDF) curves and consensus matrix were used to determine the optimal number of clusters. Survival differences between clusters were compared through Kaplan-Meier (KM) analysis using the R packages "survminer" and "survival".

2.3. Gene set enrichment analysis

The functional annotation and enrichment pathway of differentially expressed URGs were explored. Annotations for Gene Ontology (GO) categories include biological process (BP), cellular component (CC), and molecular function (MF) [18]. The Kyoto Encyclopedia of Genes and Genomes (KEGG) pathway was used exclusively to store information about gene pathways between different species [19]. The "ClusterProfiler" package was used for GO and KEGG analysis. In addition, GSVA enrichment analysis was performed to investigate functional differences between different groups [20].

2.4. Model construction and validation

The URGs related to the prognosis of HCC patients were selected using univariate Cox regression analysis. To avoid overfitting, we employed the "glmnet" R package for model optimization using the least absolute shrinkage and selection operator (LASSO) regression with 1000 iterations [21]. Using the expression values of each gene, a risk scoring formula was developed. The regression coefficients were estimated and weighted in the LASSO regression analysis. The formula for calculating the risk score was as follow:

$\sum_{i=1}^{n}(Coef_i * Exp_i)$. In the equation, *Coefi* represents the coefficients of the feature genes, while *Expi* denotes the expression levels of individual feature genes. Using the median risk score as the cutoff, patients were divided into low-risk and high-risk groups using the risk scoring formula. We assessed the disparities in survival rates between the two patient groups by utilizing the KM methond and comparing them through the log-rank examination. Principal component analysis (PCA) was employed to investigate the prognostic model's capability to accurately classify patients into distinct risk groups. Moreover, the findings were confirmed by utilizing HCC individuals from the ICGC repository. The independent prognostic value of the risk scoring was assessed using both univariate and multivariate Cox regression analyses. ROC curve analyses were conducted for 1-, 3-, and 5- years using the "survivalROC" R package, with calculation of the respective areas under the curve (AUC).

2.5. Tumor microenvironment characteristics

Within the TME, the two primary categories of non-tumor elements consisted of immune cells and stromal cells. The immune and stromal components of the TME were assessed and scored using the R package "ESTIMATE", followed by a comparison of the variances between the high-risk and low-risk cohorts. The stemness index serves as a measure that characterizes the resemblance between tumor cells and stem cells. Moreover, the correlation between risk scoring and stemness index was investigated, where mRNAsi represents an index computed using expression data and mDNAsi represents an index computed using methylation data.

2.6. Evaluation of immune cell components and immune checkpoint-related genes

Based on single-sample gene set enrichment analysis (ssGSEA), the level of immune cell infiltration and immune activity pathways of HCC patients were evaluated. The expression of immune checkpoint-related genes between high-risk and low-risk groups was further analyzed since immune checkpoints regulate immune system responses.

Analysis of somatic mutations and copy number variations.

Tumor mutational burden (TMB) refers to the quantity of genetic coding mistakes, base substitutions, and mutations in the genome, measured as the ratio per million bases [22]. The "MAF tools" R package was used to compare the differences in gene mutations between high and low-risk groups [23]. Correlation analysis was conducted to examine the relationship between TMB and risk scores. Abnormal DNA copy number variations (CNVs) were an important molecular mechanism in cancer. Therefore, we further analyzed the

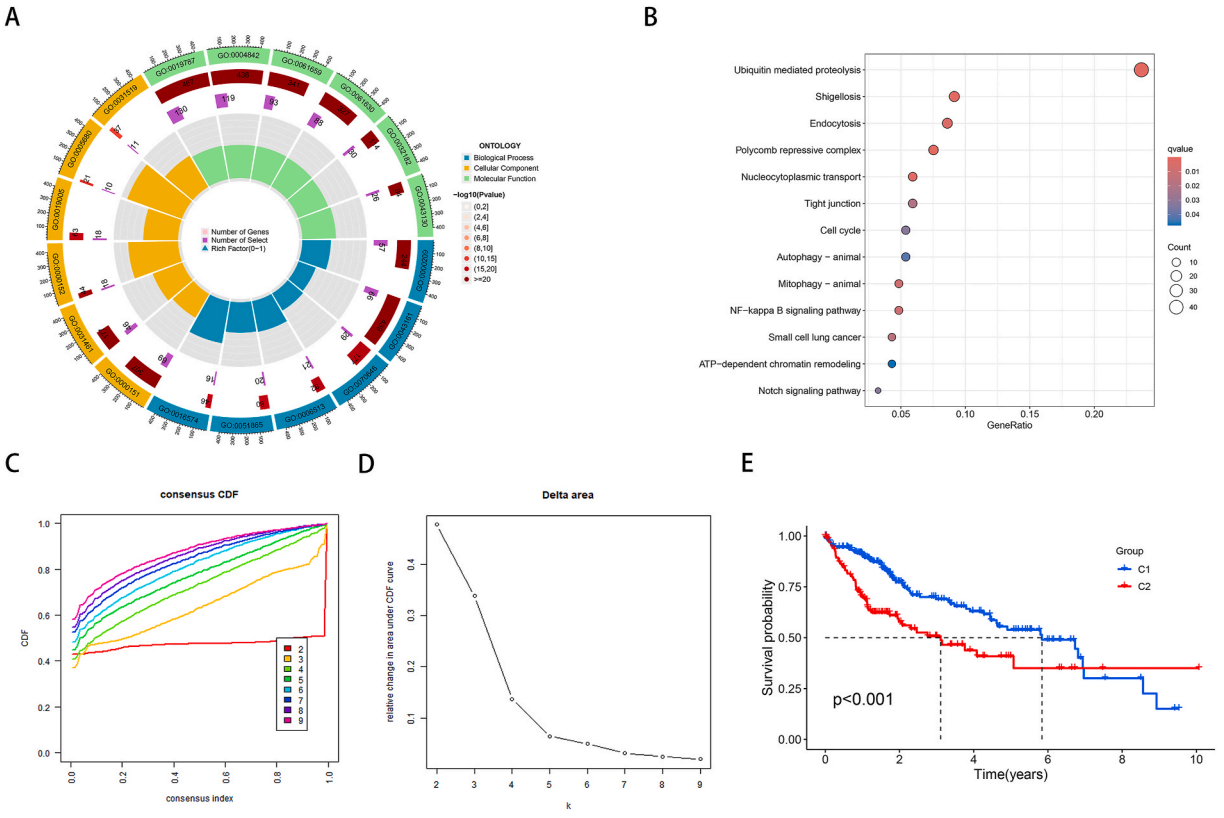

Fig. 1. Enrichment analysis of differentially expressed URGs and consistency clustering analysis. (A) GO enrichment analysis of differentially expressed URGs. (B) KEGG enrichment analysis of differentially expressed URGs. (C) Consensus clustering CDF for k = 2 to 9. (D) Relative change in area under the cumulative CDF curve for k = 2 to 9. (E) The overall survival (OS) probability of the patients in the two clusters.

Table 1
Screening of prognosis-related URGs.

gene	HR	HR.95L	HR.95H	pvalue
TRIM27	1.050561809	1.00986304	1.092900791	0.014411635
RNF2	1.264293116	1.160873553	1.376926091	7.21E-08
UBE2T	1.068071867	1.037648563	1.099387166	7.95E-06
RNF216	1.138535028	1.06168405	1.220948935	0.000274076
RNF8	1.234383139	1.071643751	1.421836066	0.003509105
ZBTB45	1.127050701	1.022824845	1.241897173	0.01570047
TRIM25	1.191995022	1.089085237	1.304628953	0.000137608
FANCD2	1.380224953	1.157404818	1.645941757	0.000334199
RNF44	1.06550795	1.031418943	1.100723619	0.000130959
PACSIN2	1.015213343	1.001399831	1.029217402	0.030765768
ZBTB40	1.50100581	1.282329277	1.756973409	4.29E-07
ARHGEF37	1.124451706	1.047276255	1.207314338	0.001223787
UIMC1	1.29136688	1.155106724	1.443700729	6.98E-06
WSB2	1.03025964	1.004584896	1.056590568	0.020600247
TRAIP	1.239661679	1.115371589	1.377801886	6.73E-05
KDM5B	1.248970549	1.084849046	1.43792119	0.001981424
RNF148	8.401541962	1.731793107	40.75885685	0.008253865
BMI1	1.113043097	1.066957807	1.161118956	6.91E-07
USP21	1.126372035	1.064617182	1.191709079	3.53E-05
NLE1	1.112408971	1.037475181	1.19275501	0.002754014
OTUB2	1.454632113	1.014448388	2.085817879	0.041552462
CHFR	1.439816664	1.091123644	1.899942356	0.009985371
DCAF16	1.127999649	1.060191916	1.200144229	0.000140195
HGS	1.061989098	1.007138505	1.119826954	0.026225242
KCTD6	1.120489664	1.05953215	1.184954216	6.72E-05
NCF2	1.036267651	1.014755381	1.058235971	0.000873189
BUB3	1.107058608	1.051188483	1.165898202	0.000118413
USP46	1.776744617	1.309977874	2.409828055	0.0002187
UBE2C	1.014649067	1.008760132	1.020572381	9.74E-07
RRP9	1.038008956	1.018178772	1.058225355	0.000150321
CUL4B	1.088278262	1.045158291	1.13317723	4.11E-05
DTL	1.065237848	1.015866608	1.117008536	0.009051041
CHAF1B	1.174273021	1.069711435	1.289055239	0.000734909
TMEM183A	1.105910219	1.03956912	1.176484939	0.001425436
ABL1	1.040318751	1.004783351	1.077110903	0.025809231
PLCG1	1.064953038	1.013965065	1.118504977	0.011937448
WDR70	1.205829597	1.054144596	1.379341148	0.006358349
NAE1	1.155849104	1.082993003	1.233606448	1.30E-05
TRIM37	1.10627399	1.035869409	1.181463735	0.002609269
ESR1	0.759499277	0.578829665	0.99656114	0.047164709
TRAF3	1.27677023	1.13181687	1.440287968	7.07E-05
ANKRD13B	1.30434736	1.120548796	1.518293573	0.000606444
BARD1	1.644364284	1.284094975	2.105711766	8.09E-05
UBE2M	1.009430177	1.001662327	1.017258266	0.017248274
LLGL1	1.18888776	1.073174838	1.317077194	0.000927247
NUP62	1.084507323	1.044981487	1.125528201	1.85E-05
CDC23	1.107073939	1.047548489	1.169981837	0.00030938
USP14	1.05294275	1.015915357	1.091319692	0.004736053
UBE2O	1.159484526	1.078363198	1.246708315	6.37E-05
RNF26	1.040280392	1.007799464	1.073808166	0.014687129
FBXL19	1.201865246	1.07206693	1.347378628	0.001613919
SRM	1.009281676	1.003806274	1.014786946	0.000872338
MAP3K9	1.507232913	1.169329961	1.942780165	0.001536048
UBE2A	1.043801464	1.008868478	1.079944036	0.013573912
WDR62	1.229804861	1.063460169	1.422168916	0.00527469
CDCA3	1.217065122	1.128314807	1.312796308	3.68E-07
WDR76	1.121822454	1.040190675	1.209860507	0.002861845
SAE1	1.026393295	1.013293542	1.039662401	7.04E-05
ZBTB39	1.414028839	1.087848311	1.838011365	0.009617715
STRN4	1.07324659	1.02961519	1.118726931	0.000843178
CUEDC1	1.05400899	1.009123937	1.100890496	0.017835254
TMUB2	1.047130009	1.009460166	1.086205571	0.013752315
SKP2	1.235358952	1.111357138	1.373196506	8.99E-05
ANAPC7	1.156730347	1.089268624	1.228370181	2.05E-06
PCGF1	1.060833192	1.005421199	1.119299117	0.030967842
FBXL7	1.121184247	1.036258252	1.213070308	0.004424646
TRIM59	1.978764583	1.397966027	2.800861538	0.000118225
POC1A	1.043822364	1.000122414	1.089431766	0.04934787

(*continued on next page*)

Table 1 (*continued*)

gene	HR	HR.95L	HR.95H	pvalue
KDM5C	1.058479433	1.018170049	1.100384667	0.004118275
NUP43	1.161749341	1.090939462	1.237155295	2.97E-06
FBXO45	1.284263228	1.133221446	1.455436662	8.89E-05
TRIM65	1.095219876	1.032047589	1.16225898	0.002694175
ZBTB41	1.078861312	1.025456251	1.135047672	0.003384986
OTUD6B	1.238260898	1.08303637	1.415732743	0.001764589
UBA2	1.024551941	1.007710153	1.041675203	0.004128279
WRAP53	1.151186715	1.021245839	1.297660958	0.02122279
SOCS2	0.80778699	0.726180641	0.898564054	8.55E-05
STAM	1.185704924	1.107780283	1.269111022	9.05E-07
SPSB2	1.076120965	1.028494261	1.12595313	0.001490878
BRCA1	1.33572832	1.128317737	1.581265707	0.000773302
WDR27	1.788219297	1.147320405	2.7871275	0.010260999
PSMD14	1.09064265	1.057531219	1.124790803	3.47E-08
DCAF13	1.110217627	1.067453596	1.154694858	1.82E-07
USP1	1.079332256	1.045944943	1.113785315	1.92E-06
SRC	1.04852851	1.018773153	1.079152933	0.001254401
ZMIZ2	1.044888406	1.013519832	1.077227842	0.004750459
MARK2	1.163010075	1.045920743	1.293207391	0.005283203
RFWD3	1.193252256	1.07841756	1.32031506	0.000621019
ATG10	1.463188165	1.124920438	1.903174247	0.004546677
GGA3	1.10302719	1.03158642	1.179415468	0.004101984
WDR45B	1.028044193	1.013222449	1.043082754	0.000189367
DCAF7	1.059467941	1.027613142	1.092310201	0.000208286
SSR3	1.027919659	1.015204665	1.040793903	1.45E-05
HDAC4	1.590905038	1.242475132	2.037045873	0.000232016
NEDD1	1.234667755	1.092230926	1.395679639	0.000750104
ING5	1.282336169	1.13337685	1.45087316	7.91E-05
WDHD1	1.483005635	1.272560944	1.728251776	4.49E-07
CDC20	1.0230007	1.015173471	1.030888279	6.52E-09
RAE1	1.169425018	1.096074443	1.247684299	2.18E-06
DPF2	1.248088671	1.112675697	1.399981445	0.000155531
KCTD2	1.067438714	1.012178044	1.125716385	0.016116498
USP39	1.110386484	1.060270552	1.162871252	8.85E-06
TRIO	1.161452003	1.036918727	1.300941646	0.009696715
PRKCI	1.127789276	1.030371257	1.234417831	0.009078812
OTUD3	1.64669298	1.138023785	2.382725041	0.008149128
KLHL17	1.216719021	1.058105454	1.399109295	0.005914345
PPP2R2C	1.137247499	1.02915801	1.256689314	0.011602421
WDR75	1.188524217	1.116259359	1.265467386	6.80E-08
UBAP2	1.319238098	1.174059114	1.482369276	3.20E-06
RNF34	1.173471559	1.086102008	1.267869399	5.07E-05
STXBP5	1.349603103	1.082751665	1.682221874	0.007646484
UBE2S	1.038148566	1.018918002	1.057742077	8.69E-05
AURKA	1.021187445	1.003972699	1.038697365	0.015647189
RNF32	4.6430039	1.690846188	12.74952468	0.002891265
PRKAA2	1.072714658	1.006485022	1.143302396	0.030868282
DNAJC6	1.168319525	1.026637532	1.329554463	0.018347574
BTBD3	1.071016354	1.014444193	1.130743355	0.013215371
PAK1IP1	1.080783394	1.047666477	1.114947144	9.95E-07
CCNF	1.405874243	1.228751591	1.608528852	7.11E-07
ASB14	12.8461937	1.208218026	136.5851933	0.0342777
WDR53	1.271731085	1.153819193	1.40169271	1.29E-06
RBBP7	1.046979475	1.019822824	1.074859275	0.000617371
WDR4	1.11588855	1.055705985	1.179501939	0.000106018
SOCS7	1.328356372	1.123861582	1.570060476	0.000871547
PJA1	1.086250947	1.040448574	1.134069621	0.000167249
TRIM16	1.046366494	1.019476141	1.073966123	0.000644687
TRIM36	2.0599438	1.369889322	3.097599487	0.000516473
UBE2Z	1.031834095	1.012396822	1.051644551	0.001238969
UBQLN4	1.033012498	1.010800498	1.0557126	0.003404854
NPLOC4	1.040593884	1.014305155	1.067563964	0.002304148
TRIM62	1.221765354	1.010182355	1.477664477	0.038981823
GGA1	1.045072281	1.007678143	1.083854085	0.017721087
SENP1	1.439151554	1.198434736	1.728218596	9.69E-05
RNF24	1.258513343	1.115151835	1.420305097	0.000194337
RNF220	1.217475886	1.106760079	1.339267255	5.23E-05
KLHL23	1.086493637	1.023574598	1.153280305	0.006419978
NUP37	1.274218292	1.148166761	1.414108394	5.12E-06

(*continued on next page*)

Table 1 (*continued*)

gene	HR	HR.95L	HR.95H	pvalue
MPP7	1.146330235	1.009870782	1.301228861	0.034698657
TBCB	1.019902655	1.006104473	1.033890071	0.00457302
RAD18	1.428740291	1.186119084	1.720989778	0.000171594
WDR12	1.357784684	1.205505707	1.529299477	4.67E-07
EED	1.300314871	1.104119018	1.531373643	0.001650241
RNFT2	1.708421896	1.183834042	2.465468362	0.00421401
WDSUB1	1.117297765	1.033403263	1.208003053	0.005352592
DTX2	1.164072942	1.040509638	1.302309719	0.007964771
NXF1	1.057068438	1.003807626	1.113155203	0.035374884
SUMO2	1.025197741	1.009118314	1.041533379	0.002033173
ANAPC1	2.342244235	1.540100553	3.562175239	6.93E-05
SACS	1.694676595	1.279072575	2.245321195	0.000238249
GTF3C2	1.196686717	1.120946288	1.277544796	7.35E-08
IFT172	1.817369645	1.372776989	2.40594973	3.00E-05
TRIM28	1.006138672	1.002340199	1.00995154	0.001518219
KCTD7	1.634848437	1.293664391	2.066014518	3.86E-05
DCAF4	1.258576749	1.038936269	1.524651203	0.018756916
SEC13	1.027542184	1.009695754	1.04570405	0.002370789

Footnotes: HR, Hazard Ratio; HR.95L, Hazard Ratio 95%CI Low; HR.95H, Hazard Ratio 95%CI High.

copy number variations of model genes.

2.7. Drug sensitivity and immunotherapy

The "oncoPredict" R package can predict drug responses and biomarkers in cancer patients from cell line screening data [24]. It generated sensitivity scores using the "oncoPredict" package to predict the median inhibitory concentration (IC50) of chemotherapeutic agents. The Tumor Immune Dysfunction and Exclusion (TIDE) score was used to assess the potential of tumor immune evasion [25]. Additionally, the immune therapy cohort IMVigor210 was utilized to evaluate the effectiveness of immunotherapy.

2.8. Data statistics

R (version 4.3.1) was utilized for conducting all statistical analyses. KM survival curves and log-rank tests were used to compare differences in survival rates between groups. Cox regression analysis was employed to assess the prognostic value of the model. ROC curves were used to evaluate model accuracy. The correlation analysis between two groups of variables was conducted using the Spearman correlation coefficient. In all tests, a p-value <0.05 was considered statistically significant.

3. Results

3.1. Selection of differential genes and clustering analysis

1330 URGs were obtained from the iUUCD database. Under the selection criteria ($|\log2\ FC| > 1$, $P < 0.05$), 443 genes were identified as differentially expressed between liver cancer tissues and normal tissues (Supplementary Fig. S1). Fig. 1A illustrated that the GO enrichment analysis revealed the enrichment of these genes in diverse pathways including protein polyubiquitination, ubiquitin ligase complex, and ubiquitin-like protein transferase activity. According to the KEGG enrichment analysis, it was found that these genes had strong connections with pathways like ubiquitin mediated proteolysis, Endocytosis, and polycomb repressive complex (Fig. 1B). Based on the CDF value and delta area value, the optimal number of clusters was determined (Fig. 1C and D). When $K = 2$, the HCC population was divided into 2 subgroups, achieving the best allocation effect (Supplementary Fig. S2). The analysis of survival indicated a notable disparity in survival rates among the two cohorts (Fig. 1E).

3.2. The construction of a prognostic model

Through Cox regression analysis, we identified 155 prognosis-related URGs (Table 1). To enhance the ability to forecast the clinical and pathological traits and outlook of patients with hepatocellular carcinoma, the LASSO regression algorithm was employed on these prognosis-associated URGs, resulting in the identification of 16 URGs for subsequent examination, determined by the minimum partial likelihood deviation (Fig. 2A and B). Fig. 2C depicted the correlation of these URGs constructed by the model. Based on the constructed model, a risk score was assigned, and using the median risk value, HCC patients were categorized into high- and low-risk groups. Fig. 2D displays the survival status of patients in the high- and low-risk groups, indicating a significantly poorer prognosis in high-risk population (Fig. 2E). PCA demonstrated that risk score effectively differentiated patients in different risk groups (Fig. 2F). Likewise, in the ICGC database, the group at high risk demonstrated a notable decline in survival, and the score for risk successfully distinguished patients of varying categories (Supplementary Figs. S3A and B). In HCC patients, the overall survival (OS) was significantly associated with clinical stage and risk score, as indicated by the univariate analysis (Fig. 3A). Furthermore, even after accounting for

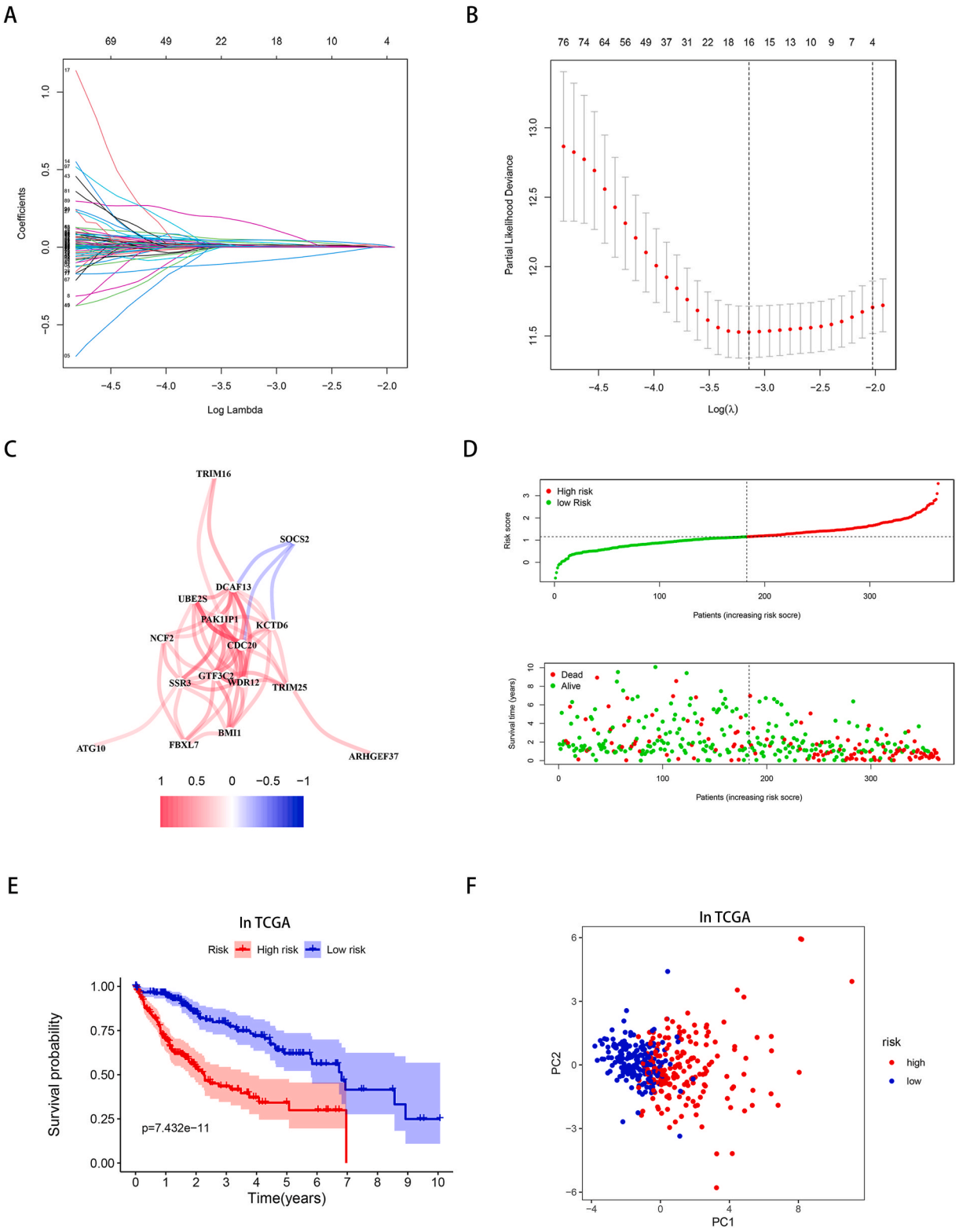

Fig. 2. Construction of prognostic model. (A) LASSO coefficient profiles of the 155 URGs. (B) LASSO cross-validation for selecting optimal tuning parameter (λ). (C) Relevance of URGs involved in model construction. (D) Distribution of risk scores and survival status between low- and high-risk groups in the TCGA Cohort. (E) Survival rate of high- and low-risk group in TCGA. (F) PCA analysis in TCGA.

clinicopathological factors including age, sex, tumor grade, and tumor stage, the risk score continued to serve as a standalone prognostic marker for patients with HCC in multifactorial analyses (Fig. 3B). The ROC curve illustrated that, compared to other clinical features, the risk score served as a strong predictor of the 1-year survival in HCC patients (Fig. 3C); similarly, it also demonstrated a strong predictive ability for the 3-year and 5-year survival (Supplementary Figs. S4A and B). In addition, risk score was strongly associated with worse pathologic grade, and higher clinical stage (Fig. 3D and E).

3.3. The tumor microenvironment and immune function

TME is crucial for the development of cancer. In the high-risk group, immune scores, stromal scores, and ESTIMATE scores were lower than in the low -risk group (Fig. 4A). In addition, we conducted a comparison of the expression of genes related to immune checkpoints and observed a high expression of genes like CTLA4 and HAVCR2 in the high-risk group (Fig. 4B). The stemness index indicated that while there was no notable association between mDNAsi and the risk score (Fig. 4C), mRNAsi exhibited a significant positive correlation with the risk score (Fig. 4D). The ssGSEA analysis demonstrated that, compared to the low-risk group, the high-risk group exhibited a significant decrease in the expression of immune cells such as NK cells, DCs, $CD8^+$ T cells, neutrophils, mast cells, and TIL (Fig. 4E). In addition, T cell stimulation, T cell inhibition, Cytolytic activity, APC inhibition, Type II IFN Reponse, and Type I IFN Reponse were significantly decreased in high-risk group, but MHC class I was increased (Fig. 4F). GSVA revealed significant enrichment of the mTOR signaling pathway, ubiquitin-mediated proteolysis, and various cancer pathways in high-risk group (Supplementary Fig. S5).

3.4. Somatic mutations and copy number variations

Additionally, somatic genetic alterations are crucial in the advancement of HCC. In high-risk group, we discovered notable alterations in TP53 (Fig. 5A), whereas low-risk group exhibited a higher prevalence of CTNNB1 mutations (Fig. 5B). There is a positive correlation between risk score and TMB (Fig. 5C). Similarly, copy number variations have a significant impact on tumor development. The copy number variants of the model genes were shown in Fig. 5D, and the locations of the model genes in the chromosomes were presented in Supplementary Fig. S6.

3.5. Drug sensitivity and immunotherapy

We examined the possible utility of chemotherapeutic drug sensitivity across various risk categories. In high-risk group, 5-Fluorouracil, Cediranib, Crizotinib, and Lapatinib had lower IC50 values (Fig. 6A–D), but Axitinib, Cisplatin, Cytarabine, Gemcitabine, and Sorafenib might display heightened sensitivity in the low-risk cohort (Supplementary Figs. S7A–E). According to the TIDE scoring, the

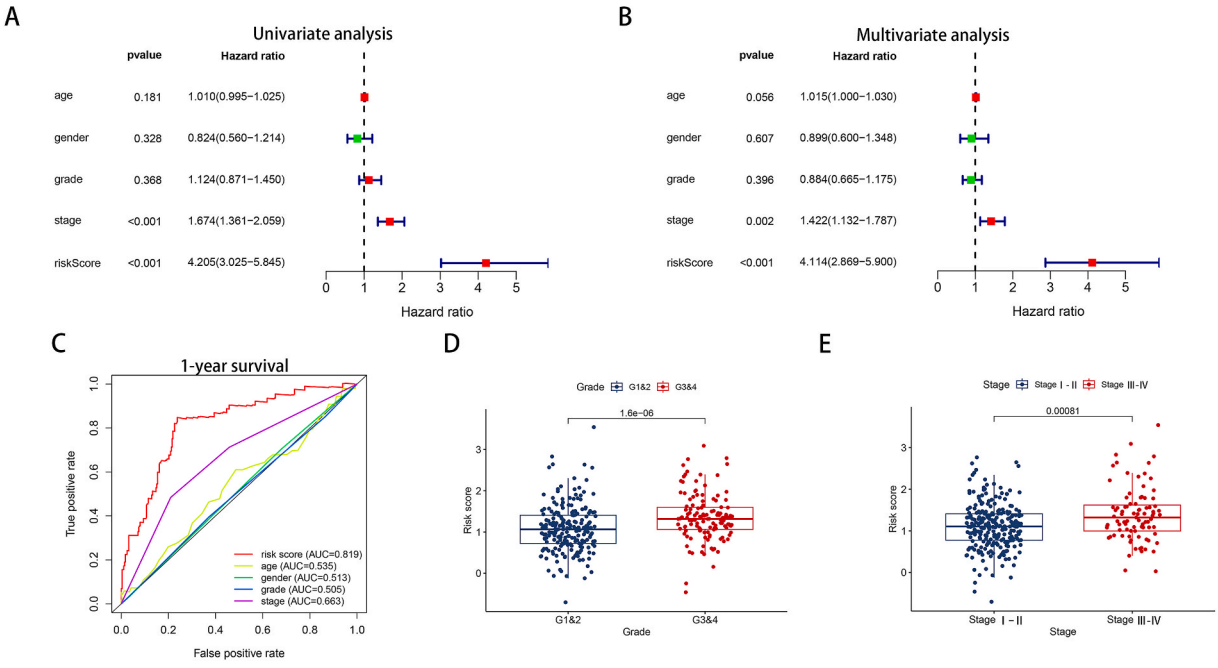

Fig. 3. Evaluation of URGs signatures as independent prognostic factors for HCC. (A) Univariate Cox regression analysis. (B) Multivariate Cox regression analysis. (C) ROC curve for 1-year survival in HCC patients. (D) The correlation between risk score and pathological grade. (E) The correlation between risk score and tumor stage.

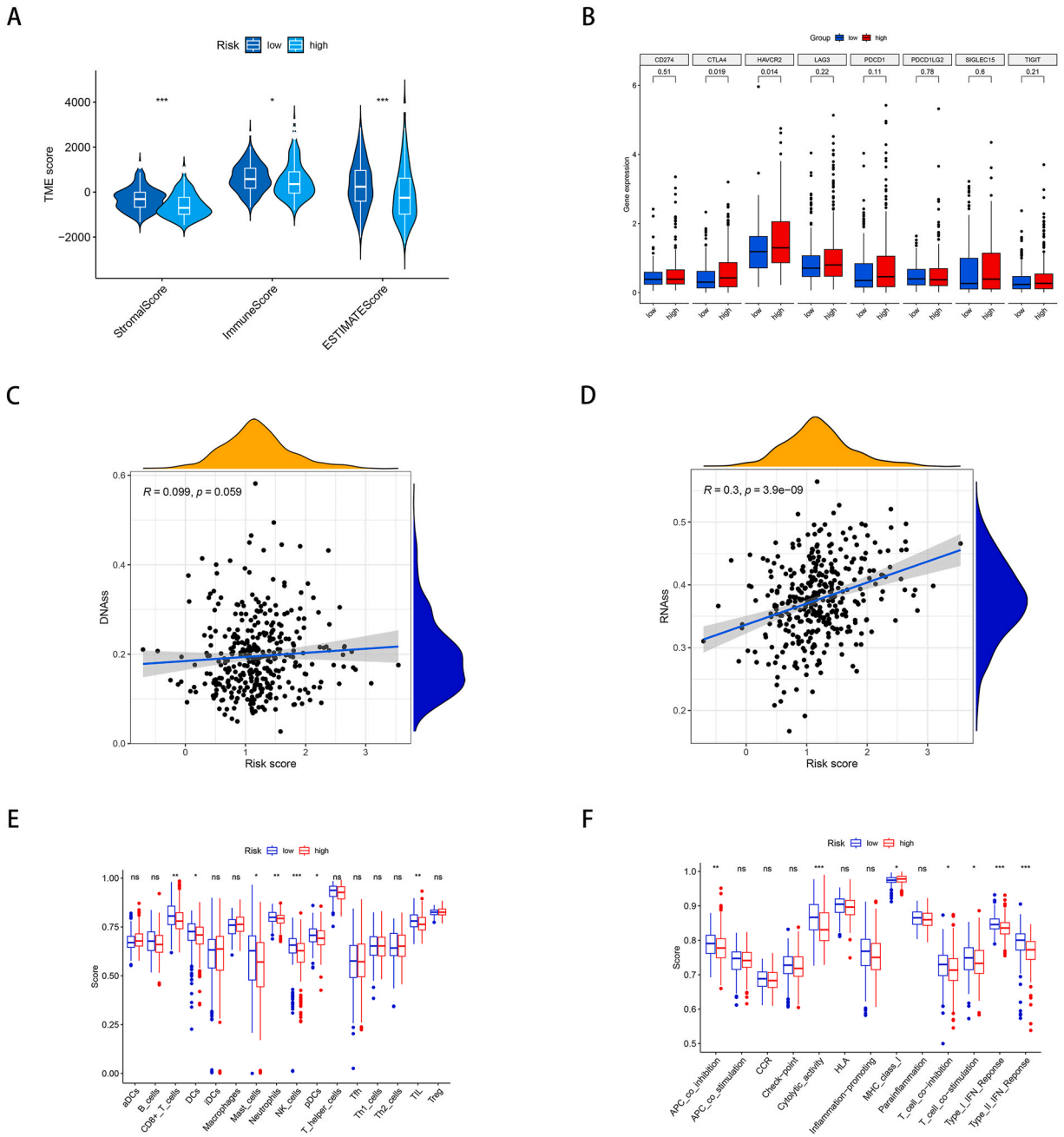

Fig. 4. (A) The TME component analysis. (B) Immune checkpoint differences between high and low risk groups. (C) association between mDNAsi and risk score. (D) association between mRNAsi and risk score. (E) The analysis of differences in immune cell infiltration between the two groups with ssGSEA. (F) The analysis of differences in immune functions between the two groups with ssGSEA.

high-risk category exhibited greater responsiveness to immunotherapy and a lower probability of immune evasion in comparison to the low-risk category (Fig. 7A). Furthermore, in the IMVigor210 immunotherapy cohort, we observed a similar trend where the high-risk group exhibited greater responsiveness to immunotherapy (Fig. 7B).

4. Discussion

HCC, a prevalent form of cancer, greatly affects the well-being of individuals [26]. Although some research has confirmed the crucial importance of tumor size, pathological grading, clinical staging, and distant metastasis in predicting patient prognosis, the establishment of prognostic markers based on the genetic level may provide a more accurate assessment of patient prognosis and guide

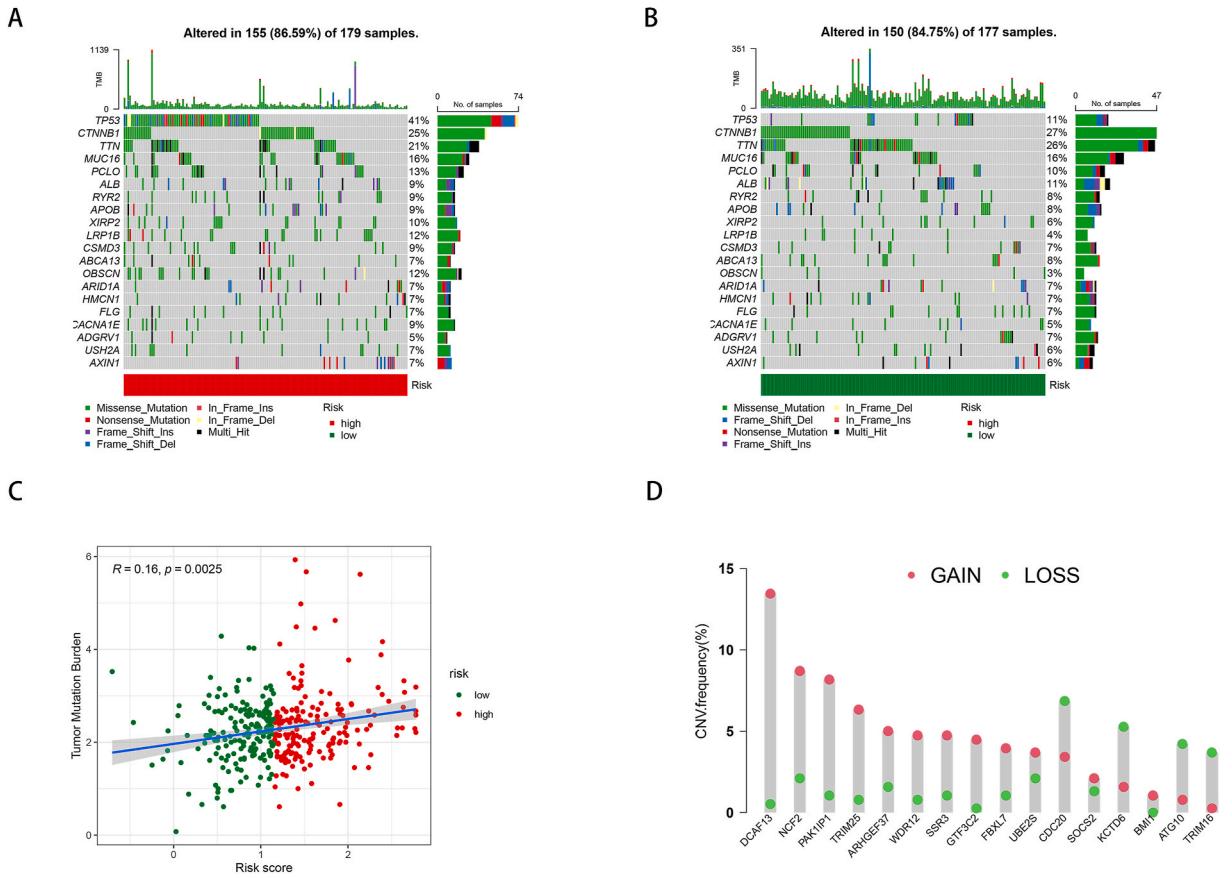

Fig. 5. (A) The somatic gene mutations in the high-risk group. (B) The somatic gene mutations in the low-risk group. (C) Correlation of risk scores with TMB. (D) The CNV gain and loss of URGs.

targeted and immune therapies for the tumor [27,28]. The occurrence and development of malignant tumors have been confirmed to be significantly influenced by protein ubiquitination, according to recent research [29,30].Therefore, we developed a predictive model utilizing URGs, which offers specific recommendations for the clinical management of patients in this research.

Using the LASSO regression technique, we discovered 16 URGs that were strongly linked to the prognosis of patients with HCC. Previous studies have confirmed that these URGs were closely associated with progression of HCC. TRIM25 has been shown to promote the growth of cancer cells through the Keap1-Nrf2 pathway [31]. Overactivation of ARHGEF37 can promote the metastasis of liver cancer [32]. BMI1 is associated with the prognosis and recurrence of liver cancer and is a new target for its treatment [33]. Liver cancer patients with elevated levels of NCF2 exhibit increased infiltration of M2 macrophages within the TME, leading to a negative prognosis [34]. High expression of SOCS2 can promote ubiquitination degradation of SLC7A11 and induce ferroptosis, affecting the sensitivity of liver cancer to radiotherapy [35]. Silencing ATG10 can suppress the growth and movement of liver tumor cells, thereby decelerating the advancement of cancer [36]. The expression of SSR3 and WDR12 is closely related to the size, differentiation degree, and clinical staging of tumors [37,38]. CDC20 protein is highly expressed in liver cancer cells and is connected to P53 mutations [39]. Lowering its expression can increase the sensitivity of liver cancer to radiotherapy [39]. Similarly, overexpression of UBE2S increases the resistance of liver cancer cells to 5-FU and oxaliplatin, serving as a prognostic marker for liver cancer patients [40]. There may be important effects of CNVs of these URGs on the function of tumor cells [41].

According to the risk score model constructed by URGs, HCC patients were divided into high-risk and low-risk groups, and the prognosis of the high-risk group was significantly lower than that of the low-risk group, which was confirmed in the ICGC database. The ROC curves confirmed that the risk score served as a reliable prognostic marker for patients with HCC, and was closely correlated with the patients' pathologic grading and clinical staging. The high-risk group had a lower level of stromal and immune cell infiltration, which was associated with a poor prognosis [42]. The imbalance of the immune microenvironment has an important impact on immune escape in hepatocellular carcinoma [43]. In addition, we found that expression of immune checkpoints CTLA4 and HAVCR2 was elevated in high-risk group. It has been reported that CTLA4 is an inhibitory immune checkpoint, and blocking CTLA4 increases anti-tumor responses [44]. In a mouse model of colorectal cancer, blocking HAVCR2 increased anti-tumor responses and promoted tumor clearance [45].

Additional research revealed a higher occurrence of TP53 mutations in the high-risk category. TP53 mutations are the most

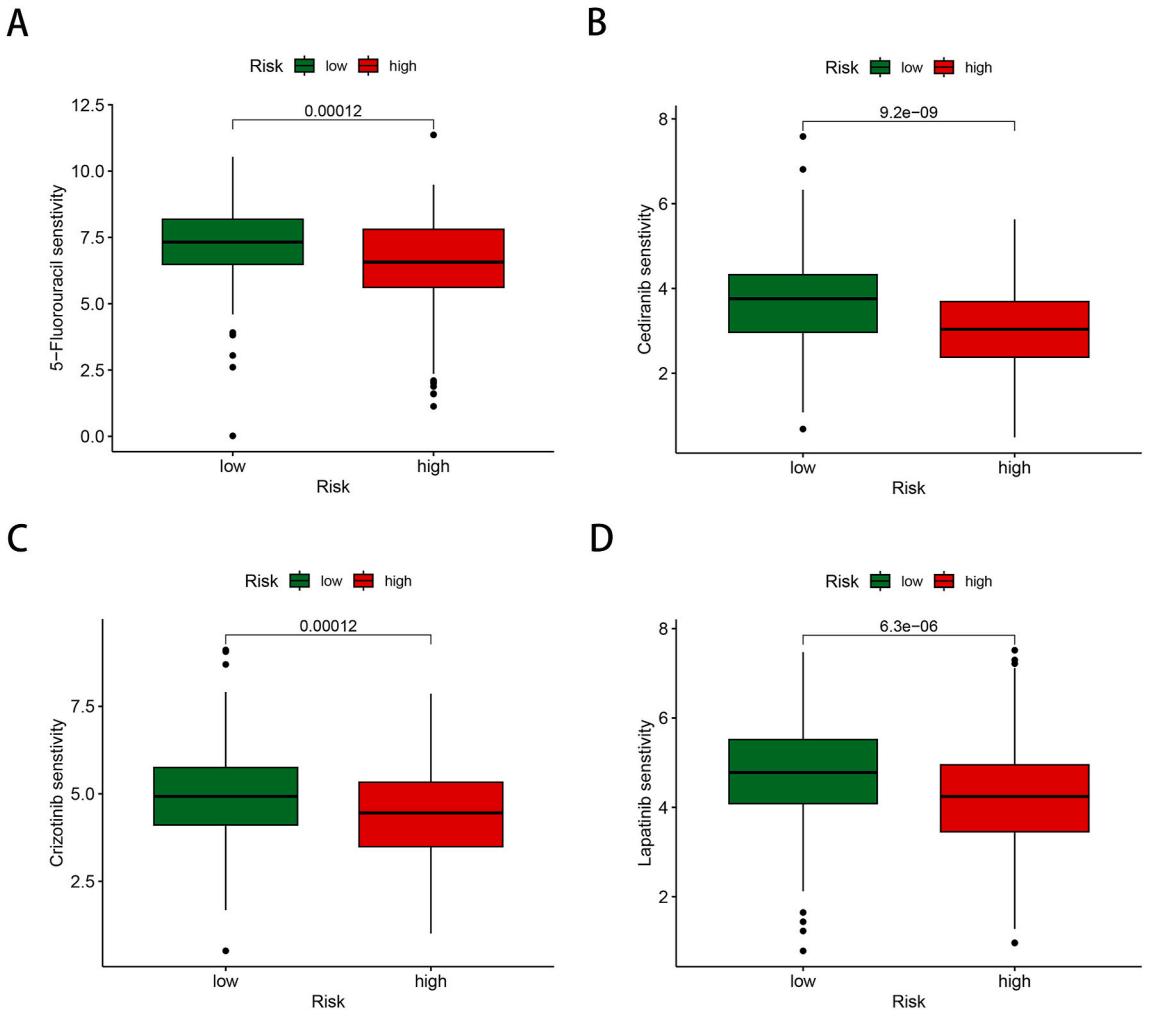

Fig. 6. Drug sensitivity analysis in the high-risk group. (A) 5-Fluorouracil. (B) Cediranib. (C) Crizotinib. (D) Lapatinib.

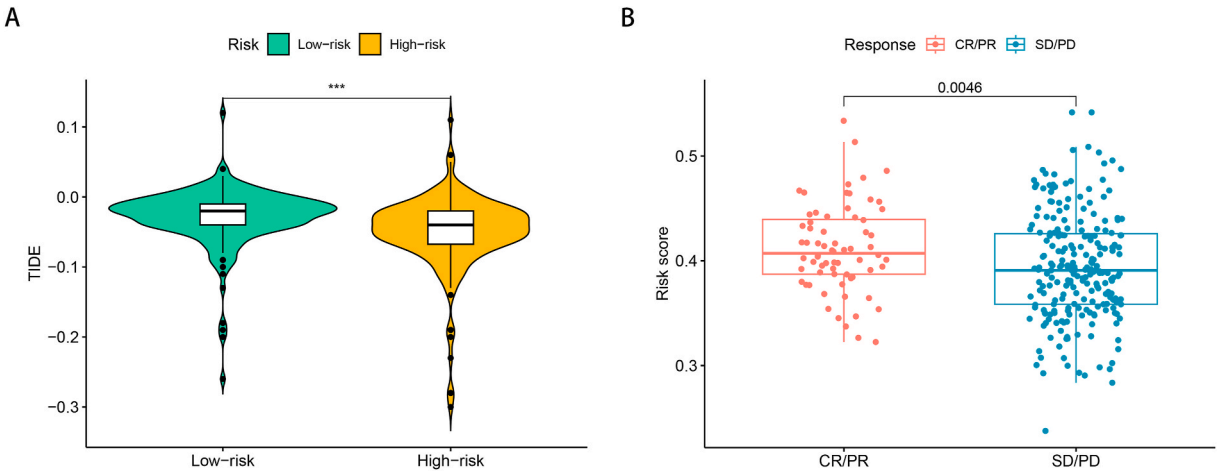

Fig. 7. Prediction of immunotherapy. (A) TIDE analysis revealing the difference of tumor immune dysfunction and exclusion in two groups. (B) Prediction immunotherapy response in IMVigor210.

common mutations in HCC, and some studies have reported that mutations in TP53 can lead to a worse prognosis for HCC patients [46,47]. However, CTNNB1 mutations were more frequent in low-risk group. CTNNB1 is a key factor in Wnt/β-catenin signaling pathway and is one of common cancer driver genes in HCC [48]. In HCC patients, CTNNB1 mutations are associated with longer survival [48]. The analysis of drug sensitivity revealed varying IC50 values in the high and low risk groups, suggesting that different chemotherapeutic agents may be appropriate for each group. TIDE scoring and the immunotherapy cohort IMVigor210 provided important guidance for immunotherapy [49,50]. Our study confirmed that people in high-risk group may have less immune evasion and higher efficacy for immunotherapy, which was consistent with some of the previous studies [51,52].

Currently, there is insufficient research on URGs in patients with liver cancer. Some previous studies have confirmed the prognostic role of URGs in certain cancers, such as pancreatic cancer and prostate cancer [53,54]. The research validated the prognostic significance of URGs in liver cancer and investigated the potential use of immunotherapy, offering valuable guidance for tailored clinical interventions. However, our study still has some limitations. Our study was based on the RNA level, and further studies at the protein level may be needed. In addition, this was a retrospective study, and prospective biological experiments and clinical studies might be needed to validate the clinical application of this risk scoring model based on URGs.

5. Conclusion

In conclusion, our study delved into molecular clustering and prognostic signals using URGs, facilitating survival prediction for HCC patients and providing guidance for their immunotherapy, potentially advancing the development of more precise treatments for liver cancer.

Ethics approval

Not applicable.

Funding

None.

Data availability statement

The public data set of this study can be found in the TCGA database (https://portal.gdc.cancer.gov/) and ICGC database (https://dcc.icgc.org/).

CRediT authorship contribution statement

Zhiyu Chen: Formal analysis, Data curation, Conceptualization. **Jing Su:** Formal analysis, Data curation, Conceptualization. **Ningning You:** Methodology. **Hong Lin:** Writing – original draft. **Shanshan Lin:** Writing – original draft. **Zhenjiang Zhang:** Writing – original draft, Data curation, Conceptualization. **Yi Chen:** Writing – review & editing, Writing – original draft, Visualization, Conceptualization.

Declaration of competing interest

The authors declare that they have no known competing financial interests or personal relationships that could have appeared to influence the work reported in this paper.

Acknowledgments

The authors thank all patients who participated in the study. Besides, the authors thank The Cancer Genome Atlas (TCGA) database for its efforts to establish and manage databases.

Appendix A. Supplementary data

Supplementary data to this article can be found online at https://doi.org/10.1016/j.heliyon.2024.e29387.

References

[1] H. Sung, J. Ferlay, R.L. Siegel, M. Laversanne, I. Soerjomataram, A. Jemal, F. Bray, Global cancer Statistics 2020: GLOBOCAN estimates of incidence and mortality worldwide for 36 cancers in 185 countries, CA Cancer J Clin 71 (3) (2021) 209–249.
[2] H. Devarbhavi, S.K. Asrani, J.P. Arab, Y.A. Nartey, E. Pose, P.S. Kamath, Global burden of liver disease: 2023 update, J. Hepatol. 79 (2) (2023) 516–537.

[3] J.M. Llovet, C.E. Willoughby, A.G. Singal, T.F. Greten, M. Heikenwälder, H.B. El-Serag, R.S. Finn, S.L. Friedman, Nonalcoholic steatohepatitis-related hepatocellular carcinoma: pathogenesis and treatment, Nat. Rev. Gastroenterol. Hepatol. 20 (8) (2023) 487–503.
[4] T.H. Yang, C. Chan, P.J. Yang, Y.H. Huang, M.H. Lee, Genetic susceptibility to hepatocellular carcinoma in patients with chronic hepatitis virus infection, Viruses 15 (2) (2023).
[5] A. Forner, M. Reig, J. Bruix, Hepatocellular carcinoma, Lancet 391 (10127) (2018) 1301–1314.
[6] K.N. Swatek, D. Komander, Ubiquitin modifications, Cell Res. 26 (4) (2016) 399–422.
[7] X. Zhou, S.C. Sun, Targeting ubiquitin signaling for cancer immunotherapy, Signal Transduct Target Ther 6 (1) (2021) 16.
[8] Z. Ge, J.S. Leighton, Y. Wang, X. Peng, Z. Chen, H. Chen, Y. Sun, F. Yao, J. Li, H. Zhang, J. Liu, C.D. Shriver, H. Hu, H. Piwnica-Worms, L. Ma, H. Liang, Integrated genomic analysis of the ubiquitin pathway across cancer types, Cell Rep. 23 (1) (2018) 213–226.e3.
[9] L. Zhang, Z. Shi, F. Zhang, B. Chen, W. Qiu, L. Cai, X. Lin, Ubiquitination-related biomarkers in metastatic melanoma patients and their roles in tumor microenvironment, Front. Oncol. 13 (2023) 1170190.
[10] X. Huang, V.M. Dixit, Drugging the undruggables: exploring the ubiquitin system for drug development, Cell Res. 26 (4) (2016) 484–498.
[11] E.M. Swisher, K.K. Lin, A.M. Oza, C.L. Scott, H. Giordano, J. Sun, G.E. Konecny, R.L. Coleman, A.V. Tinker, D.M. O'Malley, R.S. Kristeleit, L. Ma, K.M. Bell-McGuinn, J.D. Brenton, J.M. Cragun, A. Oaknin, I. Ray-Coquard, M.I. Harrell, E. Mann, S.H. Kaufmann, A. Floquet, A. Leary, T.C. Harding, S. Goble, L. Maloney, J. Isaacson, A.R. Allen, L. Rolfe, R. Yelensky, M. Raponi, I.A. McNeish, Rucaparib in relapsed, platinum-sensitive high-grade ovarian carcinoma (ARIEL2 Part 1): an international, multicentre, open-label, phase 2 trial, Lancet Oncol. 18 (1) (2017) 75–87.
[12] G. Wang, F. Bie, X. Qu, X. Yang, S. Liu, Y. Wang, C. Huang, K. Wang, J. Du, Expression profiling of ubiquitin-related genes in LKB1 mutant lung adenocarcinoma, Sci. Rep. 8 (1) (2018) 13221.
[13] Y. Li, L. An, Z. Jia, J. Li, E. Zhou, F. Wu, Z. Yin, W. Geng, T. Liao, W. Xiao, J. Deng, W. Chen, M. Li, Y. Jin, Identification of ubiquitin-related gene-pair signatures for predicting tumor microenvironment infiltration and drug sensitivity of lung adenocarcinoma, Cancers 14 (14) (2022).
[14] Z. Wang, S. Cheng, Y. Liu, R. Zhao, J. Zhang, X. Zhou, W. Shu, D. Feng, H. Wang, Gene signature and prognostic value of ubiquitination-related genes in endometrial cancer, World J. Surg. Oncol. 21 (1) (2023) 3.
[15] T. Lv, B. Zhang, C. Jiang, Q. Zeng, J. Yang, Y. Zhou, USP35 promotes hepatocellular carcinoma progression by protecting PKM2 from ubiquitination-mediated degradation, Int. J. Oncol. 63 (4) (2023).
[16] H. Zhang, P. Xia, Z. Yang, J. Liu, Y. Zhu, Z. Huang, Z. Zhang, Y. Yuan, Cullin-associated and neddylation-dissociated 1 regulate reprogramming of lipid metabolism through SKP1-Cullin-1-F-box(FBXO11) -mediated heterogeneous nuclear ribonucleoprotein A2/B1 ubiquitination and promote hepatocellular carcinoma, Clin. Transl. Med. 13 (10) (2023) e1443.
[17] M.D. Wilkerson, D.N. Hayes, ConsensusClusterPlus: a class discovery tool with confidence assessments and item tracking, Bioinformatics 26 (12) (2010) 1572–1573.
[18] Gene Ontology Consortium: going forward, Nucleic Acids Res. 43 (Database issue) (2015) D1049–D1056.
[19] M. Kanehisa, M. Furumichi, M. Tanabe, Y. Sato, K. Morishima, KEGG: new perspectives on genomes, pathways, diseases and drugs, Nucleic Acids Res. 45 (D1) (2017) D353–d361.
[20] S. Hänzelmann, R. Castelo, J. Guinney, GSVA: gene set variation analysis for microarray and RNA-seq data, BMC Bioinf. 14 (2013) 7.
[21] Q. Yuan, J. Ren, Z. Wang, L. Ji, D. Deng, D. Shang, Identification of the real hub gene and construction of a novel prognostic signature for pancreatic adenocarcinoma based on the weighted gene Co-expression network analysis and least absolute shrinkage and selection operator algorithms, Front. Genet. 12 (2021) 692953.
[22] Z.R. Chalmers, C.F. Connelly, D. Fabrizio, L. Gay, S.M. Ali, R. Ennis, A. Schrock, B. Campbell, A. Shlien, J. Chmielecki, F. Huang, Y. He, J. Sun, U. Tabori, M. Kennedy, D.S. Lieber, S. Roels, J. White, G.A. Otto, J.S. Ross, L. Garraway, V.A. Miller, P.J. Stephens, G.M. Frampton, Analysis of 100,000 human cancer genomes reveals the landscape of tumor mutational burden, Genome Med. 9 (1) (2017) 34.
[23] A. Mayakonda, D.C. Lin, Y. Assenov, C. Plass, H.P. Koeffler, Maftools: efficient and comprehensive analysis of somatic variants in cancer, Genome Res. 28 (11) (2018) 1747–1756.
[24] D. Maeser, R.F. Gruener, R.S. Huang, oncoPredict: an R package for predicting in vivo or cancer patient drug response and biomarkers from cell line screening data, Brief Bioinform 22 (6) (2021).
[25] P. Jiang, S. Gu, D. Pan, J. Fu, A. Sahu, X. Hu, Z. Li, N. Traugh, X. Bu, B. Li, J. Liu, G.J. Freeman, M.A. Brown, K.W. Wucherpfennig, X.S. Liu, Signatures of T cell dysfunction and exclusion predict cancer immunotherapy response, Nat Med 24 (10) (2018) 1550–1558.
[26] J. Hartke, M. Johnson, M. Ghabril, The diagnosis and treatment of hepatocellular carcinoma, Semin. Diagn. Pathol. 34 (2) (2017) 153–159.
[27] G.P. Nagaraju, B. Dariya, P. Kasa, S. Peela, B.F. El-Rayes, Epigenetics in hepatocellular carcinoma, Semin. Cancer Biol. 86 (Pt 3) (2022) 622–632.
[28] C. Shen, W. Chai, J. Han, Z. Zhang, X. Liu, S. Yang, Y. Wang, D. Wang, F. Wan, Z. Fan, H. Hu, Identification and validation of a dysregulated TME-related gene signature for predicting prognosis, and immunological properties in bladder cancer, Front. Immunol. 14 (2023) 1213947.
[29] L. Chen, S. Liu, Y. Tao, Regulating tumor suppressor genes: post-translational modifications, Signal Transduct Target Ther 5 (1) (2020) 90.
[30] Y. Xu, W. Wu, Q. Han, Y. Wang, C. Li, P. Zhang, H. Xu, Post-translational modification control of RNA-binding protein hnRNPK function, Open Biol 9 (3) (2019) 180239.
[31] Y. Liu, S. Tao, L. Liao, Y. Li, H. Li, Z. Li, L. Lin, X. Wan, X. Yang, L. Chen, TRIM25 promotes the cell survival and growth of hepatocellular carcinoma through targeting Keap1-Nrf2 pathway, Nat. Commun. 11 (1) (2020) 348.
[32] X. Zhang, L. Ren, J. Wu, R. Feng, Y. Chen, R. Li, M. Wu, M. Zheng, X.G. Wu, W. Luo, H. He, Y. Huang, M. Tang, J. Li, ARHGEF37 overexpression promotes extravasation and metastasis of hepatocellular carcinoma via directly activating Cdc42, J. Exp. Clin. Cancer Res. 41 (1) (2022) 230.
[33] R. Wang, H. Fan, M. Sun, Z. Lv, W. Yi, Roles of BMI1 in the initiation, progression, and treatment of hepatocellular carcinoma, Technol. Cancer Res. Treat. 21 (2022) 15330338211070689.
[34] N. Huang, J. Zhang, S. Kuang, Z. Li, H. Zhao, J. Wu, M. Liu, L. Wang, Role of NCF2 as a potential prognostic factor and immune infiltration indicator in hepatocellular carcinoma, Cancer Med. 12 (7) (2023) 8991–9004.
[35] Q. Chen, W. Zheng, J. Guan, H. Liu, Y. Dan, L. Zhu, Y. Song, Y. Zhou, X. Zhao, Y. Zhang, Y. Bai, Y. Pan, J. Zhang, C. Shao, SOCS2-enhanced ubiquitination of SLC7A11 promotes ferroptosis and radiosensitization in hepatocellular carcinoma, Cell Death Differ. 30 (1) (2023) 137–151.
[36] F. Li, K. Li, D. Li, W. Zhang, K.W. Yang, D. Ke, Q. Guo, R.S. Shi, ATG10 overexpression is related to the dismal prognosis and promotes the growth and migration of hepatocellular carcinoma cells via cyclin B1/CDK1 and CDK2, Am. J. Cancer Res. 13 (4) (2023) 1188–1208.
[37] S. Huang, W. Zhong, Z. Shi, K. Wang, H. Jin, Z. Zhang, H. Wang, Y. Wei, S. Chen, Q. Zhou, X. He, Overexpression of signal sequence receptor γ predicts poor survival in patients with hepatocellular carcinoma, Hum. Pathol. 81 (2018) 47–54.
[38] Y. Yin, L. Zhou, R. Zhan, Q. Zhang, M. Li, Identification of WDR12 as a novel oncogene involved in hepatocellular carcinoma propagation, Cancer Manag. Res. 10 (2018) 3985–3993.
[39] S. Zhao, Y. Zhang, X. Lu, H. Ding, B. Han, X. Song, H. Miao, X. Cui, S. Wei, W. Liu, S. Chen, J. Wang, CDC20 regulates the cell proliferation and radiosensitivity of P53 mutant HCC cells through the Bcl-2/Bax pathway, Int. J. Biol. Sci. 17 (13) (2021) 3608–3621.
[40] L. Gui, S. Zhang, Y. Xu, H. Zhang, Y. Zhu, L. Kong, UBE2S promotes cell chemoresistance through PTEN-AKT signaling in hepatocellular carcinoma, Cell Death Discov 7 (1) (2021) 357.
[41] T. Becchi, L. Beltrame, L. Mannarino, E. Calura, S. Marchini, C. Romualdi, A pan-cancer landscape of pathogenic somatic copy number variations, J Biomed Inform 147 (2023) 104529.
[42] L. Pan, J. Fang, M.Y. Chen, S.T. Zhai, B. Zhang, Z.Y. Jiang, S. Juengpanich, Y.F. Wang, X.J. Cai, Promising key genes associated with tumor microenvironments and prognosis of hepatocellular carcinoma, World J. Gastroenterol. 26 (8) (2020) 789–803.
[43] X. Hao, G. Sun, Y. Zhang, X. Kong, D. Rong, J. Song, W. Tang, X. Wang, Targeting immune cells in the tumor microenvironment of HCC: new opportunities and challenges, Front. Cell Dev. Biol. 9 (2021) 775462.

[44] R. Xing, J. Gao, Q. Cui, Q. Wang, Strategies to improve the antitumor effect of immunotherapy for hepatocellular carcinoma, Front. Immunol. 12 (2021) 783236.
[45] Y.H. Huang, C. Zhu, Y. Kondo, A.C. Anderson, A. Gandhi, A. Russell, S.K. Dougan, B.S. Petersen, E. Melum, T. Pertel, K.L. Clayton, M. Raab, Q. Chen, N. Beauchemin, P.J. Yazaki, M. Pyzik, M.A. Ostrowski, J.N. Glickman, C.E. Rudd, H.L. Ploegh, A. Franke, G.A. Petsko, V.K. Kuchroo, R.S. Blumberg, CEACAM1 regulates TIM-3-mediated tolerance and exhaustion, Nature 517 (7534) (2015) 386–390.
[46] J. Long, A. Wang, Y. Bai, J. Lin, X. Yang, D. Wang, X. Yang, Y. Jiang, H. Zhao, Development and validation of a TP53-associated immune prognostic model for hepatocellular carcinoma, EBioMedicine 42 (2019) 363–374.
[47] S. Ling, Q. Shan, Q. Zhan, Q. Ye, P. Liu, S. Xu, X. He, J. Ma, J. Xiang, G. Jiang, X. Wen, Z. Feng, Y. Wu, T. Feng, L. Xu, K. Chen, X. Zhang, R. Wei, C. Zhang, B. Cen, H. Xie, P. Song, J. Liu, S. Zheng, X. Xu, USP22 promotes hypoxia-induced hepatocellular carcinoma stemness by a HIF1α/USP22 positive feedback loop upon TP53 inactivation, Gut 69 (7) (2020) 1322–1334.
[48] Z. Wang, Y.Y. Sheng, X.M. Gao, C.Q. Wang, X.Y. Wang, X.U. Lu, J.W. Wei, K.L. Zhang, Q.Z. Dong, L.X. Qin, β-catenin mutation is correlated with a favorable prognosis in patients with hepatocellular carcinoma, Mol Clin Oncol 3 (4) (2015) 936–940.
[49] S. Zhao, L. Wang, W. Ding, B. Ye, C. Cheng, J. Shao, J. Liu, H. Zhou, Crosstalk of disulfidptosis-related subtypes, establishment of a prognostic signature and immune infiltration characteristics in bladder cancer based on a machine learning survival framework, Front. Endocrinol. 14 (2023) 1180404.
[50] J. Li, H. Qiao, F. Wu, S. Sun, C. Feng, C. Li, W. Yan, W. Lv, H. Wu, M. Liu, X. Chen, X. Liu, W. Wang, Y. Cai, Y. Zhang, Z. Zhou, Y. Zhang, S. Zhang, A novel hypoxia- and lactate metabolism-related signature to predict prognosis and immunotherapy responses for breast cancer by integrating machine learning and bioinformatic analyses, Front. Immunol. 13 (2022) 998140.
[51] T. Wang, L. Dai, S. Shen, Y. Yang, M. Yang, X. Yang, Y. Qiu, W. Wang, Comprehensive molecular analyses of a macrophage-related gene signature with regard to prognosis, immune features, and biomarkers for immunotherapy in hepatocellular carcinoma based on WGCNA and the LASSO algorithm, Front. Immunol. 13 (2022) 843408.
[52] X. Qi, J. Guo, G. Chen, C. Fang, L. Hu, J. Li, C. Zhang, Cuproptosis-related signature predicts the prognosis, tumor microenvironment, and drug sensitivity of hepatocellular carcinoma, J Immunol Res 2022 (2022) 3393027.
[53] Y. Guo, Z. Wu, K. Cen, Y. Bai, Y. Dai, Y. Mai, K. Hong, L. Qu, Establishment and validation of a ubiquitination-related gene signature associated with prognosis in pancreatic duct adenocarcinoma, Front. Immunol. 14 (2023) 1171811.
[54] G. Song, Y. Zhang, H. Li, Z. Liu, W. Song, R. Li, C. Wei, T. Wang, J. Liu, X. Liu, Identification of a ubiquitin related genes signature for predicting prognosis of prostate cancer, Front. Genet. 12 (2021) 778503.